

UDK/UDC: 544.272:551.51(078.7)

Prejeto/Received: 26.09.2024

Izvorni znanstveni članek – *Original scientific paper*

Sprejeto/Accepted: 06.01.2025

DOI: [10.15292/acta.hydro.2024.08](https://doi.org/10.15292/acta.hydro.2024.08)

Objavljeno na spletu/Published online: 03.03.2025

NUMERICAL STUDY OF HIGHLY EFFICIENT CENTRIFUGAL CYCLONES

NUMERIČNA ŠTUDIJA VISOKOUČINKOVITIH CENTRIFUGALNIH CIKLONOV

Murodil Madaliev¹, Zokhidjon Abdulkhaev^{1,*}, Yunusali Khusanov¹, Saxiba Mirzababayeva¹,
Zebuniso Abobakirova¹

¹ Fergana Polytechnic Institute, Fergana, Uzbekistan

Abstract

Centrifugal cyclones have been developed for centuries to treat process streams, but their efficiency in removing fine dust remains below 80%. The widespread use of cyclones in various industries is the result of their simplicity in design and their reliable operation. However, the process occurring inside a cyclone is a complex scientific problem that still remains unsolved within the framework of aerohydraulics, as evidenced by the variety of cyclone designs. The current level of cyclone cleaning's efficiency for process streams does not meet sanitary standards and significantly affects the level of environmental pollution. This paper compares various configurations of centrifugal cyclones, including cyclones without screws, with a screw of a uniform pitch, and with a screw of a variable pitch to regulate the twist of the flow. Numerical simulations were performed using the Comsol Multiphysics 5.6 software package using the SST turbulence model. The obtained numerical data show that the efficiency of a cyclone with a variable screw pitch is significantly higher than that of cyclones without screws and with a screw of a uniform pitch.

Keywords: cyclone, mathematical modeling, turbulence models, Reynolds-averaged Navier–Stokes equations.

Izveček

Centrifugalni cikloni se že stoletja razvijajo za obdelavo procesnih tokov, vendar njihova učinkovitost pri odstranjevanju drobnega prahu ostaja pod 80 %. Široka uporaba ciklonov v različnih panogah je posledica njihove preproste zasnove in zanesljivega delovanja. Proces znotraj ciklonov je zapleten znanstveni problem in v okviru aerohidromehanike ostaja nerešen, kar dokazuje raznolikost modelov. Trenutna raven učinkovitosti ciklonskega čiščenja procesnih tokov ne ustreza sanitarnim standardom in bistveno vpliva na onesnaženost okolja. Članek primerja različne konfiguracije centrifugalnih ciklonov, vključno s cikloni brez vijakov, z vijakom enakomernega koraka in z vijakom spremenljivega koraka, ki uravnava zasuk toka. Numerične simulacije so bile izvedene z uporabo programskega paketa Comsol Multiphysics 5.6 z uporabo modela

* Stik / Correspondence: zokhidjon@ferpi.uz

© Madaliev M. et al.; This is an open-access article distributed under the terms of the [Creative Commons Attribution – NonCommercial – ShareAlike 4.0 Licence](https://creativecommons.org/licenses/by-nc-sa/4.0/).

© Madaliev M. et al.; Vsebina tega članka se sme uporabljati v skladu s pogoji [licence Creative Commons Priznanje avtorstva – Nekomercialno – Deljenje pod enakimi pogoji 4.0](https://creativecommons.org/licenses/by-nc-sa/4.0/).

turbulence SST. Dobljeni numerični podatki kažejo, da je izkoristek ciklona z vijakom spremenljivega koraka bistveno večji kot pri ciklonih brez vijakov in cikloni z vijakom enakomernega koraka.

Ključne besede: ciklon, matematično modeliranje, turbulenčni modeli, Reynoldsovo povprečene Navier-Stokesove enačbe.

1. Introduction

Gas cyclones are devices that use the vortex effect to separate the dispersed phase (dust) from the continuous phase (gas). These devices are widely used for collecting solid particles from gas streams and have been used in various industries for many years. Cyclones are popular due to their simple design, low operating costs, lack of moving parts, high reliability, and ability to operate in harsh environments. When a gas cyclone is on, vortex centrifugal forces act on every point inside the device, which leads to the separation of the dispersed phase, being heavier, and its movement towards the walls of the cyclone. These particles are then driven downwards by axial velocity towards the collector, where they are gathered. The purified air is then vortexed upward again and leaves the cyclone through the outlet pipe. Although the operating principle behind a gas cyclone seems very simple, the physics governing the liquid flow inside the device makes for a complex and not yet fully understood area.

The wide variety of applications of cyclone separators has led many researchers to study the effect of cyclone size on performance and flow field.

Studies conducted by Hoffmann et al. (2001), Xiang and Lee (2005), Zhu and Lee (1999), Avci and Karagoz (2003), Chuah et al. (2006), and Surmen et al. (2011) provide valuable data on the influence of various parameters on the operation of gas cyclones. In particular, research data indicate the importance of the length and height of the cyclone, as well as the geometry of the conical tip, on its effectiveness. Although the works of Hoffman and Xiang present different results on the effect of cyclone length, the studies of Zhu et al. highlight the importance of cyclone pitch on separation efficiency. These inconsistencies may be explained by differences in methodology and experimental conditions. The mathematical model developed by Avsiev et al.

provides a new tool for predicting the efficiency of cyclones and agrees well with experimental data. In addition, the work of Chuah et al. confirms that CFD computer modelling can accurately reproduce the performance of gas cyclones, allowing for more accurate predictions. The research of Surmen et al. (2011), based on a theoretical approach, is also important because it predicts the cutoff size of a cyclone based on its geometry and fluid properties. Overall, these works make significant contributions to the understanding of the physics and optimization of gas cyclones, which has important implications for their application in various industrial processes.

Studies by Lee et al. (2006) and Hsu et al. (2014) add to our knowledge of the influence of various parameters on the performance of gas cyclones. In particular, they emphasize the importance of the length of the cone and cylinder, as well as other geometric parameters. The work of Lee et al. (2006), which doubled the length of the cyclone cone compared to the Stairmand model, revealed instability of the flow field and incomplete development of flow in the cylinder region as a result of the abrupt transition to the conical segment. These results highlight the importance of an optimal cylinder-to-cone-length ratio for efficient cyclone operation. Experiments by Hsu et al. (2014), covering different cyclone geometries, including cylinder and cone lengths, revealed a decrease in pressure drop and an increase in aerosol penetration with increasing these parameters. However, detailed data on flow field variables were not presented, which may limit the understanding of the mechanisms underlying these changes. Overall, these studies highlight the importance of considering various geometric parameters when designing and optimizing gas cyclones, as well as the need for further research to better understand the physical processes occurring within these devices.

Indeed, there is limited literature examining the effect of cyclone length on cyclone performance.

Most published work on cyclone length is based on comparing the increase in cylinder or cone length using a standard cyclone model. However, these results are often not applicable to each other due to differences in cyclone models and experimental conditions. Comparing the effects of geometric changes in specific cyclone models (Kuznetsov et al., 2009) operating under similar conditions is extremely important for understanding the effect of cyclone length on its performance. This approach will eliminate the influence of factors not related to geometric changes and more accurately determine the influence of the cyclone length on its operation (Tarasova, 2010). Thus, future research in this area should pay particular attention to comparing geometric changes in specific cyclone models under similar operating conditions to provide more accurate and comparable results.

To eliminate the shortcomings inherent in classical centrifugal cyclones, article (Zlochevskiy and Mukhopad, 2015) proposes to use a new type of cyclone for cleaning process air. The highly efficient centrifugal cyclone is equipped with a conical screw insert housed in a perforated, truncated cone. This creates a confined space in the form of a helical channel with a decreasing cross-sectional area. In this case, the exhaust pipe limits the interaction between the main flow, containing dust particles, and the counterflow, containing purified air.

As part of this work, the effect of a flow swirling screw on the cyclone's efficiency was investigated. This new approach can improve the efficiency of cleaning air from dust and other pollutants, which can lead to improved working conditions in various industrial processes. However, to fully understand the benefits and evaluate the effectiveness of this new type of cyclone, additional research and experimental testing of its operation under various operating conditions is required.

2. Physical formulation of the problem

The proposed device operates on the following principle (see Fig. 1a): a mixture of dust and air enters the device along a tangent line from above and begins to move downward, rotating between the

conical and cylindrical parts. After this, the cone moves into a second, larger cone, where the particles begin to move toward the cone's wall. A vortex is formed in the center of the cyclone, capable of carrying small particles into the bunker. To prevent this effect, a reverse cone is installed at the bottom of the device. To more effectively capture small particles, it is necessary to increase the centrifugal speed inside the cyclone. For this purpose, a screw is installed inside the cyclone, as shown in Fig. 1b. The pitch of the auger in Fig. 1b is fixed. However, Fig. 1c shows a modification where the screw's pitch is gradually reduced, which leads to a further increase in the rotation speed of the particles inside the cyclone.

Details of the studied cyclones are given in Table 1, corresponding to Fig. 2.

2.1 Mathematical formulation of the problem

The present study uses numerical simulation to predict the flow field variables, pressure drop, and collection efficiency. The Navier–Stokes equations are discretized using the finite element method (FEM). The choice of a particular turbulence model depends on the nature of the flow, the available hardware resources, and its ability to capture the complete physics of fluid flow. To model Reynolds stresses in RANS equations, Comsol Multiphysics 5.6 (COMSOL Inc. Retrieved, 2015) provides various closure models; the SST model was used in this work. SST models are very robust turbulence models suitable for most engineering and industrial flows.

To study the flow dynamics, consider a system of hydrodynamic equations. In this case, we will make the assumption that the volume density of particles in the main flow zone is negligible compared to the gas flow density. Indeed, in real cyclones, the dust density does not exceed 5 g/m^3 , the air density is 1.29 kg/m^3 , and the particle density is 2700 kg/m^3 . However, the density of dust near the wall due to accumulation can greatly exceed this indicator. But this happens in a rather narrow layer, whose size can be neglected in comparison with the characteristic parameters of the cyclone.

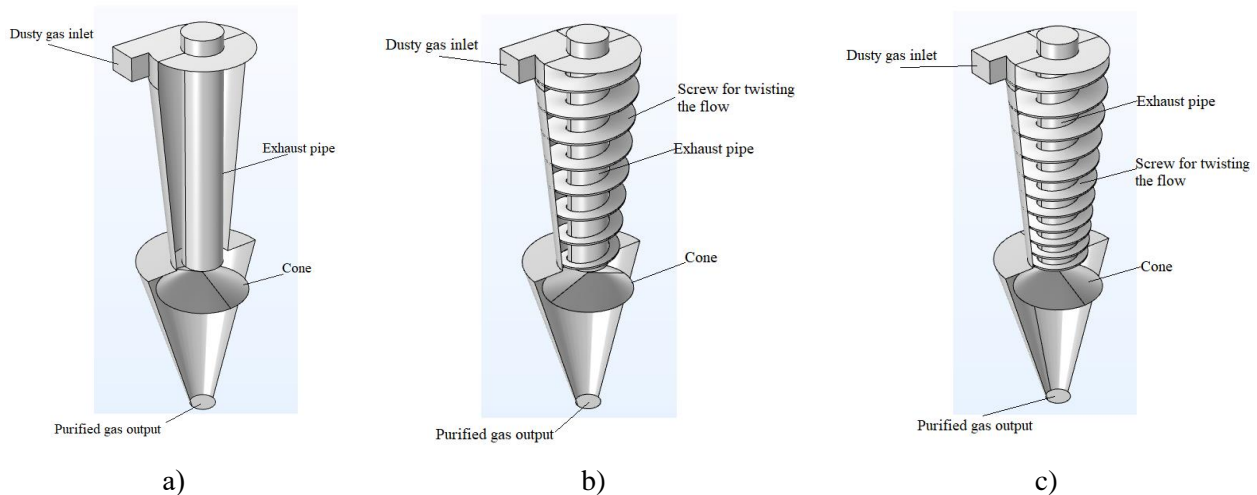


Figure 1: Highly efficient centrifugal cyclones: a) without a screw cyclone, b) a screw cyclone with a uniform screw pitch, c) a screw cyclone with a variable screw pitch.

Slika 1: Visokoučinkoviti centrifugalni cikloni: a) brez vijaka, b) z vijakom enakomernega koraka, c) z vijakom spremenljivega koraka.

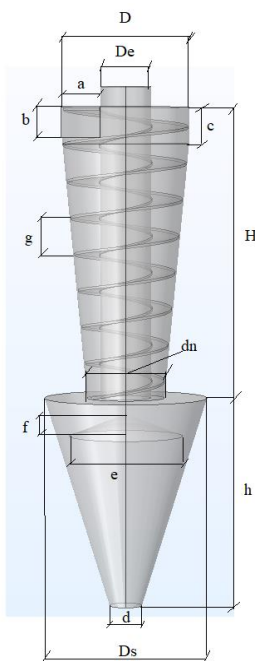


Figure 2: Details of the studied cyclones.

Slika 2: Podrobnosti preučevanih ciklonov.

To numerically study the problem posed, a system of Reynolds-averaged Navier–Stokes equations is used (Malikov and Madaliev, 2020; Son and Murodil, 2020). The system of equations does not take into account the forces due to the effects of turbulent migration, namely Seffman, Magnus (lift), and Coriolis, because they are significantly less than

Table 1: Dimensions of high-efficiency cyclones.

Preglednica 1: Mere ciklonov z visokim izkoristkom.

Dimen sions	Dimensionle ss ratio (Size)/D 1- cyclone	Dimension less ratio (Size)/D 2- cyclone	Dimension less ratio (Size)/D 3- cyclone
D	D	D	D
De	0.4D	0.4D	0.4D
C	0.3D	0.3D	0.3D
H	2.4D	2.4D	2.4D
h	1.7D	1.7D	1.7D
a	0.25D	0.25D	0.25D
b	0.3D	0.3D	0.3D
e	0.92D	0.92D	0.92D
f	0.2D	0.2D	0.2D
d	0.25D	0.25D	0.25D
Ds	1.3D	1.3D	1.3D
g	-	0.3D	0.3D≈0.15 D
dn	0.3D	0.3D	0.3D

the centrifugal force. Thus, for mathematically modelling the processes of transfer of dust particles and aerosols in dust collectors, it is sufficient to take into account centrifugal, gravitational, and Stokes forces.

$$\left\{ \begin{array}{l} \rho \nabla \mathbf{u} = 0, \\ \rho \frac{d\mathbf{u}}{dt} = -\nabla p + \mu_{eff} \nabla^2 \mathbf{u} + \rho \mathbf{g}, \\ \rho \frac{d\mathbf{u}_p}{dt} = k_m (\mathbf{u} - \mathbf{u}_p), \\ \mu_{eff} = \mu + \mu_T. \end{array} \right. \quad (1)$$

here \mathbf{u} – is the air flow velocity vector; \mathbf{u}_p – similar velocity vectors for the n th fraction of dust; ρ – gas density; μ, μ_T – molecular and turbulent viscosities, p – hydrostatic pressure, \mathbf{g} – acceleration of gravity.

The interaction coefficient between phases was determined through the Stokes parameter:

$$k_m = \frac{18\mu}{\rho_p \delta_m^2}. \quad (2)$$

here ρ_p represents the density of the dust particles' material, and δ_m denotes the 'effective' diameter of the particles.

2.2 Turbulence models

Menter's shear stress transport (SST) model is a combination of the k - ϵ and k - ω models. In this scheme, k - ω is used for the wall layer, while k - ϵ is used for the outer region. This combination allows the flow features both near the wall and in the outer regions to be taken into account, providing more accurate modeling of turbulent flows. The SST model is currently very popular and is widely included in many CFD programs. Its efficiency and accuracy make it the preferred choice for modeling shear stress transfer in a variety of applications. It is important to note that the SST model provides effective tools for modeling turbulent flows and has been successfully used in various hydrodynamic calculation packages. Its ability to account for flow patterns both within the wall layer and in external regions makes it a valuable tool for engineers and researchers involved in analyzing and modeling complex turbulent flows.

$$\left\{ \begin{array}{l} \frac{dk}{dt} = \nabla[(v + \sigma_k v_i) \nabla k] + P - \beta^* \omega k, \\ \frac{d\omega}{dt} = \nabla[(v + \sigma_\omega v_i) \nabla \omega] + \frac{\gamma}{v_i} P - \beta \omega^2 + 2(1 - F_1) \frac{\sigma_{\omega 2}}{\omega} \nabla \omega \nabla k. \end{array} \right. \quad (3)$$

Here k is the specific turbulent kinetic energy ($\text{m}^2 \text{s}^{-2}$) and ω is the specific rate of turbulent dissipation (s^{-1}). Additional data are presented in studies by Menter (1994), Smirnov and Menter (2009), and Spalart and Rumsey (2007). These works contain details and extended information about other meanings.

2.3 Solution method

COMSOL Multiphysics 5.6 provides several effective solvers for problems of various physical phenomena (Agullo et al., 2013; Kuzmin et al., 2012). When choosing a suitable solver, it is important to consider the type of physics being modeled, the complexity of the problem, the required accuracy, and the available computational resources. To solve the equations of a two-phase turbulent model, the Segregated method with the PARDISO direct solver algorithm was used in this work. This method allows the interaction of various physical processes in the system to be taken into account by solving the systems of linear equations arising at each step of the iterative method. To accelerate convergence, the Newton iterative method with a damping factor of 0.1 was used. The iterative process was used for nonlinear equations, where, at each iteration, the linear systems were solved using the PARDISO algorithm. The calculations were continued for up to 250 iterations with a specified tolerance factor of 1 and a residual factor of 1000. The tolerance factor (1) specifies the accuracy of the solution for each iteration, and the residual factor (1000) indicates the maximum permissible level of discrepancy between the calculated and exact values. These parameters are necessary to control the convergence of the iterative method to ensure a balance between the computational load and the accuracy of the result. These parameters were tuned to the required accuracy and specificity of the problem, ensuring an efficient and reliable solution to the turbulent model equations within the framework of the software used. The computational experiment was carried out

at flow rate $U_0 = 18 \text{ m/s}$. Particle sizes are taken in the range from 0.2 to 10 microns. Solid particles are injected using the normal surface condition at a speed equal to the speed of the fluid entering the cyclone. Particles reaching the cyclone's walls collide with it and are reflected back. For the condition of low dust load, it is quite reasonable to assume that the collision of discrete phase particles with the walls of the cyclone is ideally elastic, wherefore the recovery coefficients in both the tangential and normal directions of the wall are taken as unity. The total density of the solid phase at the inlet was equal and distributed uniformly over the cross section. Fig. 3 shows a grid diagram for calculating cyclones. Table 2 provides complete information about the computational normal grid. To ensure convergence to the accurate solution, a mesh independence study was conducted using the grids presented in Fig. 3. Specifically, we compared the axial and tangential velocity profiles obtained from the coarse, normal, and fine grids. The results showed negligible differences between the normal and fine grids, confirming that the normal grid provided a solution close to the converged and accurate result.

2.4 Checking the model's adequacy

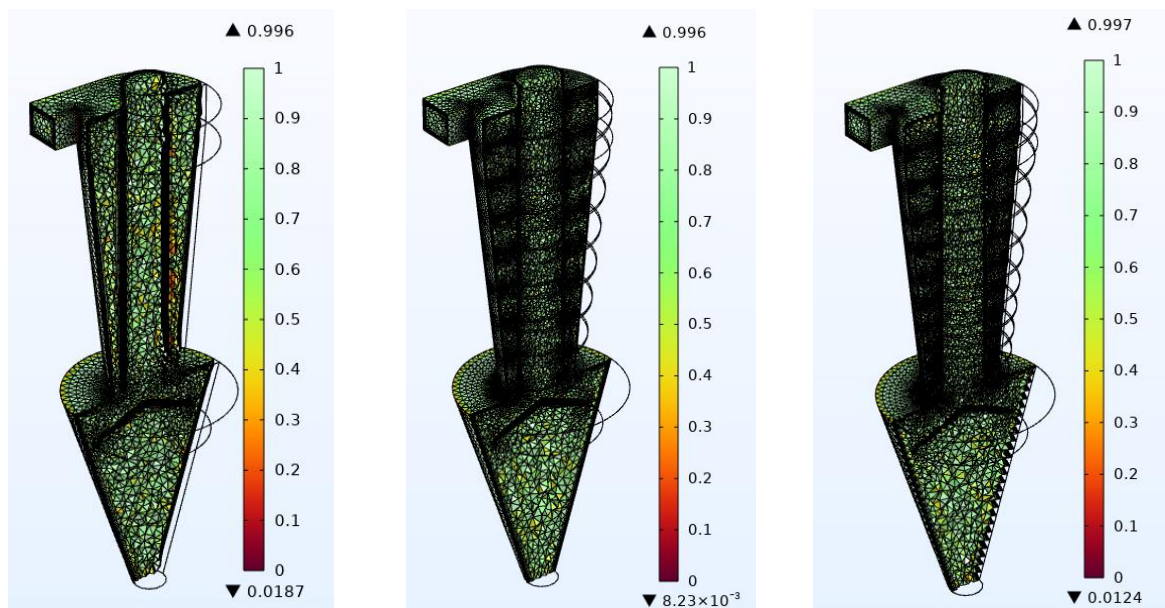


Figure 3: Normal grids for calculating cyclones.

Slika 3: Normalne mreže za izračun ciklonov.

Since the process within a centrifugal cyclone involves complex turbulent dynamics, testing the model's adequacy before applying it to describe the process in a new cyclone is an important step. The Stairmand cyclone, for which experimental data is available, is considered in this context. This allows you to compare the results of numerical simulations with real measurements and evaluate the model's accuracy. To obtain complete information about the initial conditions and design of the Stairmand cyclone, it is recommended to refer to the relevant sources indicated in the articles (Brar et al., 2015; Hoekstra, 2000 and Wei et al., 2017), where an experimental study of this device was carried out.

Fig. 4 shows the average axial and tangential velocities at $z=217.5 \text{ mm}$ from the cyclone roof with experimental values (Hoekstra, 2000).

As can be seen from Fig. 4, the result obtained from the SST model is in good agreement with the experimental results. Therefore, this model can be used for our cyclone.

2.5. Calculation results and their discussion

Fig. 5 shows contour plots of the average axial velocity of cyclones in the midplane.

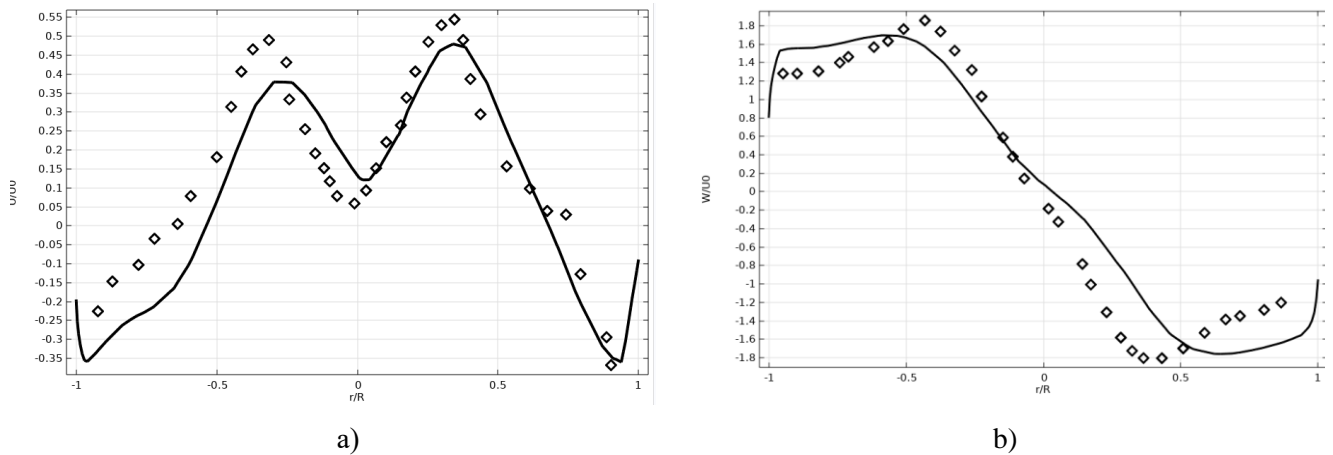


Figure 4: The average axial a) and tangential b) velocities at $z=217.5$ mm from the cyclone roof are represented by experimental values (Hoekstra, 2000).

Slika 4: Povprečne aksialne a) in tangencialne b) hitrosti pri $z = 217,5$ mm od strehe ciklona so predstavljene z eksperimentalnimi vrednostmi (Hoekstra, 2000).

Table 2: Provides complete information about the computational normal grid.

Preglednica 2: Celostne informacije o računski normalni mreži.

	without a screw cyclone	a screw cyclone with a uniform screw pitch	a screw cyclone with a variable screw pitch
Mesh vertices	82873	522 786	535 099
Tetrahedra	214 572	1 309 184	1 364 717
Pyramids	3546	43 880	56 624
Prisms	86 436	537 442	524 384
Triangles	13 552	105 106	119 532
Quads	318	390	348
Edge elements	860	7063	7853
Vertex element	26	96	101
Number of elements	304 554	1 890 506	1 945 725
Minimum element quality	0.01873	0.006998	0.005481
Average element quality	0.6853	0.6758	0.6627
Element volume ratio	7.451E-6	1.668E-5	7.667E-6
Mesh volume mm ³	6.642E7	6.481E7	6.431E7

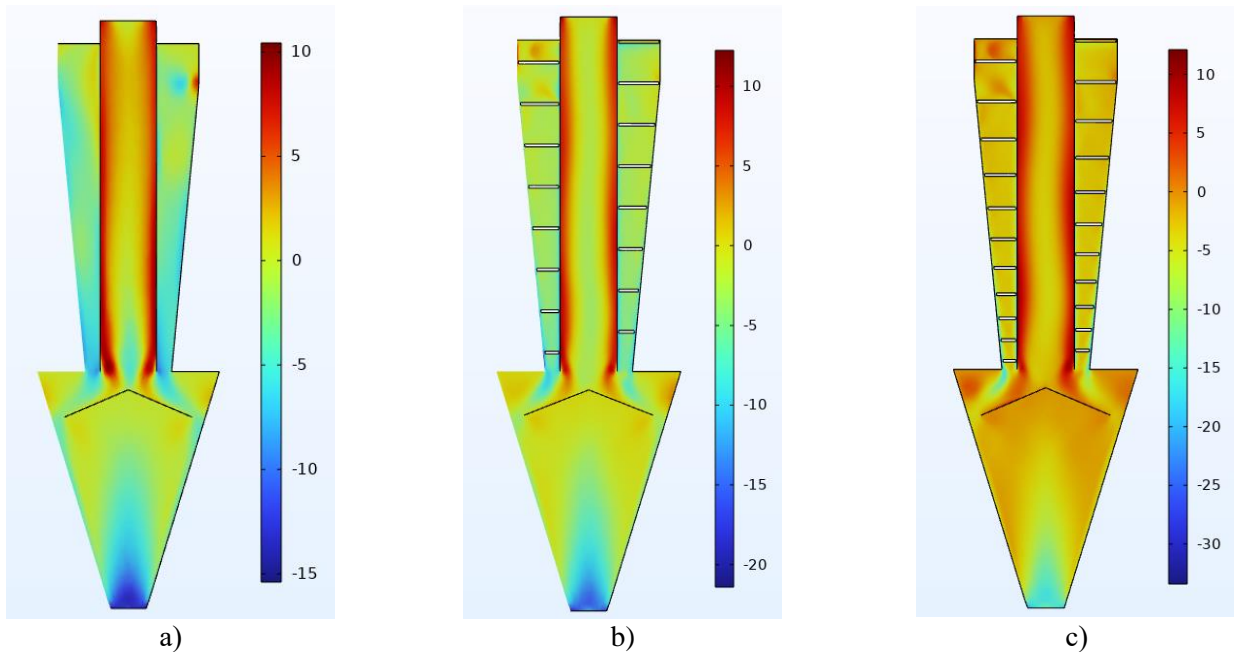


Figure 5: Isolines of the velocity field in cyclones [m/s]: a) without a screw cyclone, b) a screw cyclone with a uniform screw pitch, c) a screw cyclone with a variable screw pitch.

Slika 5: Izolinije hitrostnega polja v ciklonih [m/s]: a) brez vijaka, b) z vijakom enakomernega koraka, c) z vijakom spremenljivega koraka.

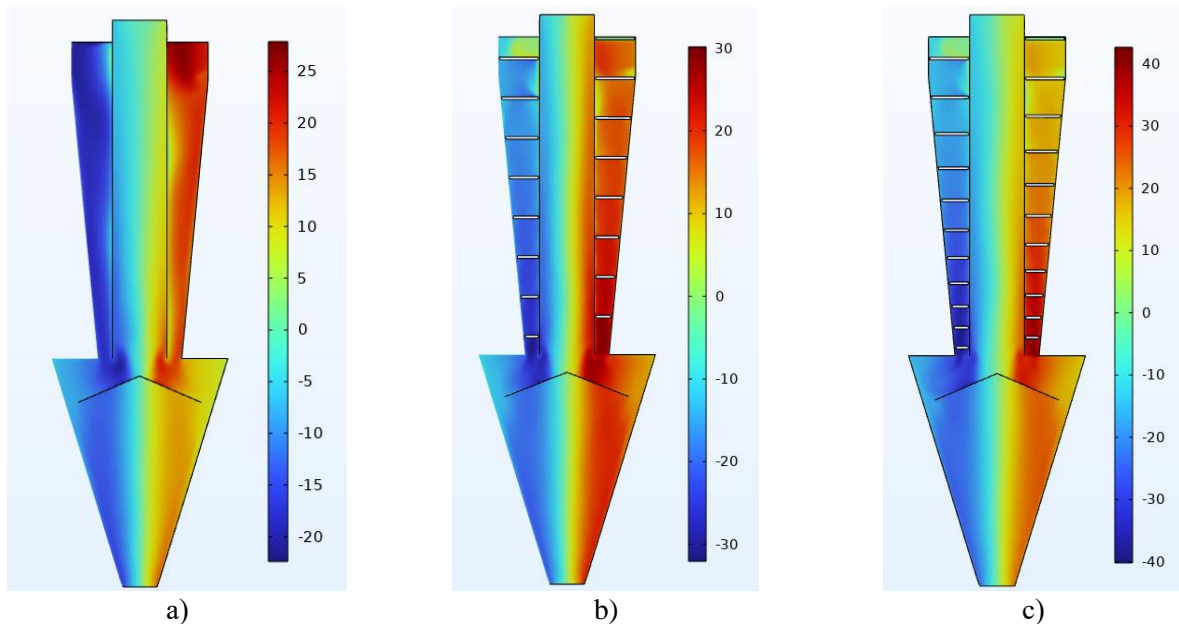


Figure 6: Isolines of the tangential velocity field in cyclones [m/s]: a) without a screw cyclone, b) a screw cyclone with a uniform screw pitch, c) a screw cyclone with a variable screw pitch.

Slika 6: Izolinije tangencialnega hitrostnega polja v ciklonih [m/s]: a) brez vijaka, b) z vijakom enakomernega koraka, c) z vijakom spremenljivega koraka.

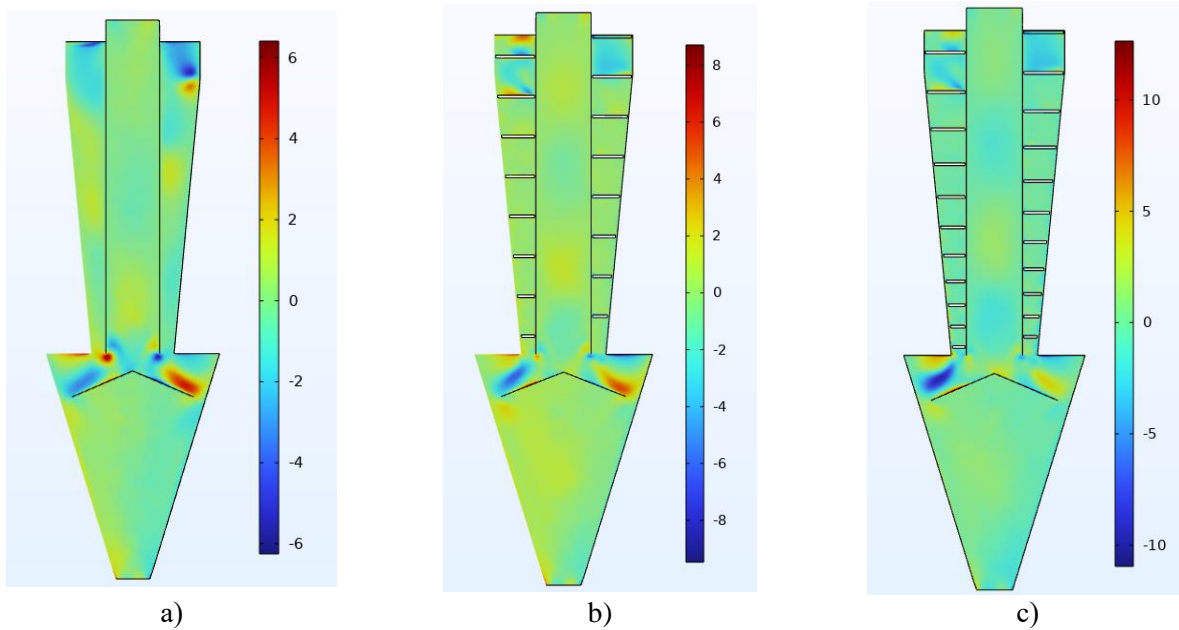


Figure 7: Isolines of the radial velocity field in cyclones [m/s]: a) without a screw cyclone, b) a screw cyclone with a uniform screw pitch, c) a screw cyclone with a variable screw pitch.

Slika 7: Izolinije radialnega hitrostnega polja v ciklonih [m/s]: a) brez vijaka, b) z vijakom enakomernega koraka, c) z vijakom spremenljivega koraka.

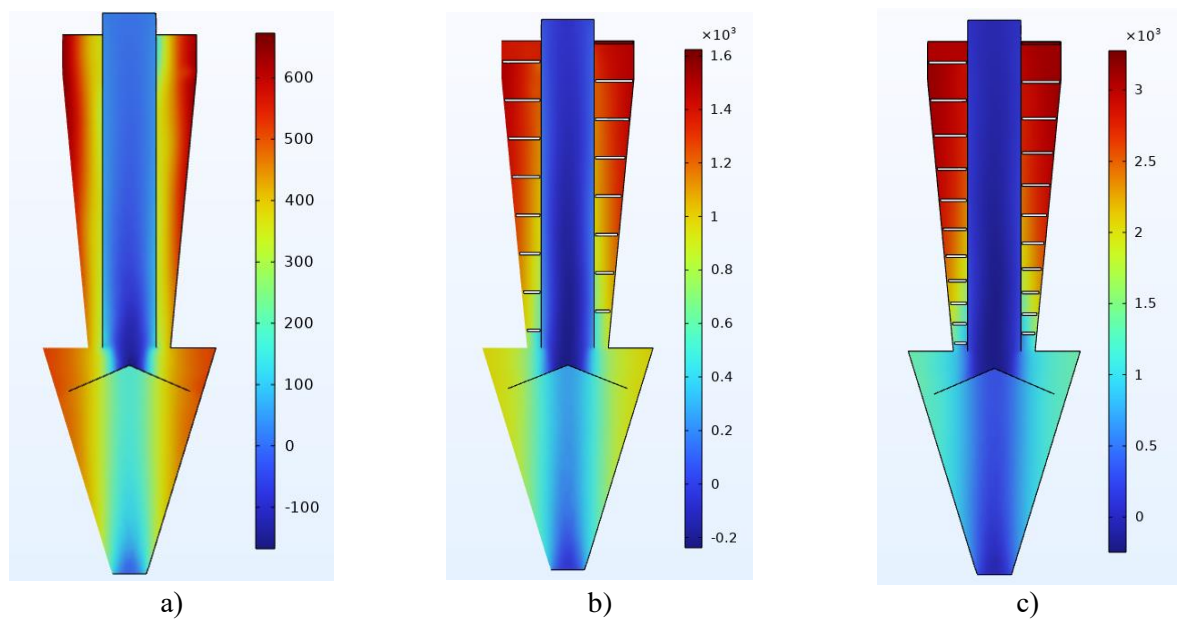


Figure 8: Isolines of the pressure field in cyclones [Pa]: a) without a screw cyclone, b) a screw cyclone with a uniform screw pitch, c) a screw cyclone with a variable screw pitch.

Slika 8: Izolinije tlačnega polja v ciklonih [Pa]: a) brez vijaka, b) z vijakom enakomernega koraka, c) z vijakom spremenljivega koraka.

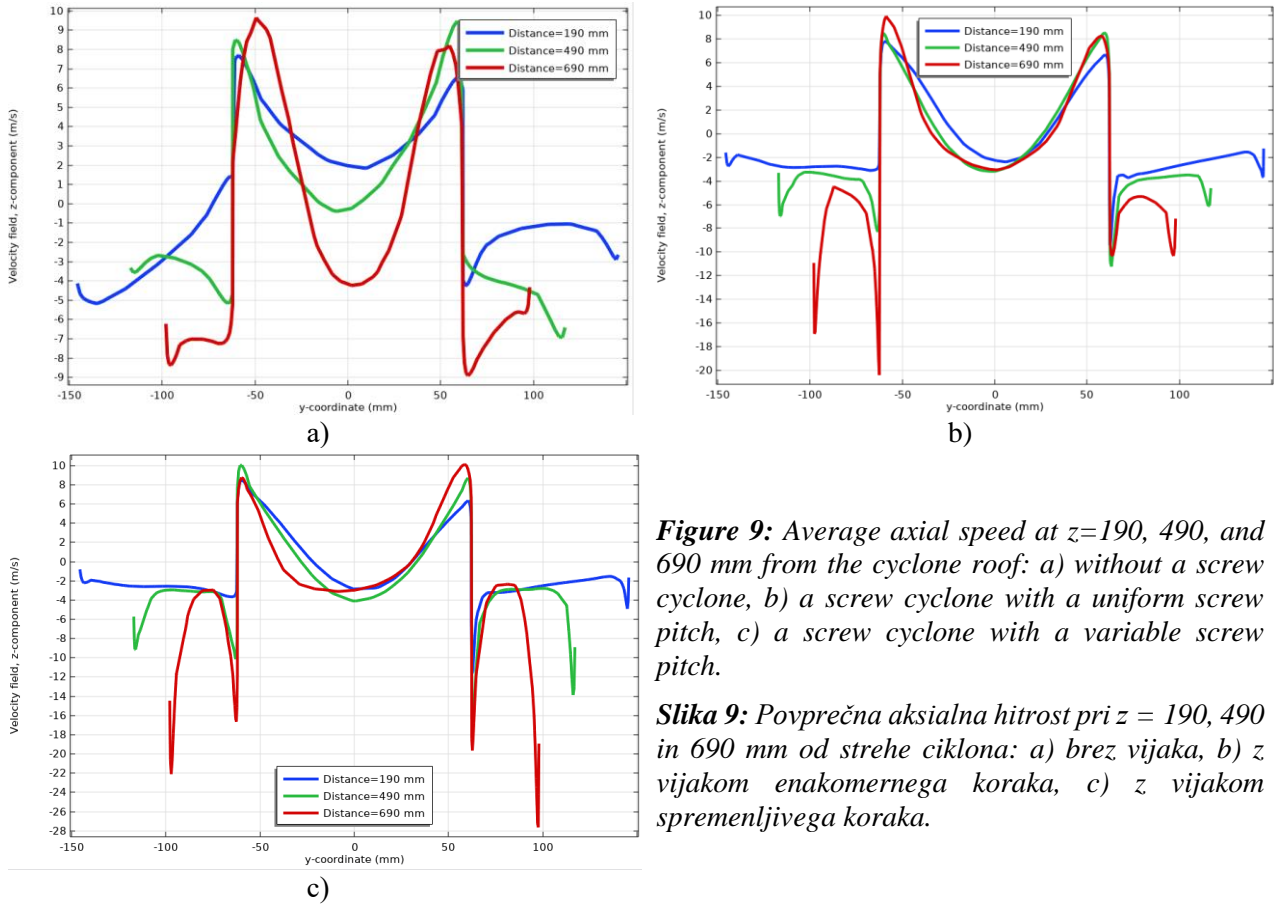


Figure 9: Average axial speed at $z=190, 490,$ and 690 mm from the cyclone roof: a) without a screw cyclone, b) a screw cyclone with a uniform screw pitch, c) a screw cyclone with a variable screw pitch.

Slika 9: Povprečna aksialna hitrost pri $z = 190, 490$ in 690 mm od strehe ciklona: a) brez vijaka, b) z vijakom enakomernega koraka, c) z vijakom spremenljivega koraka.

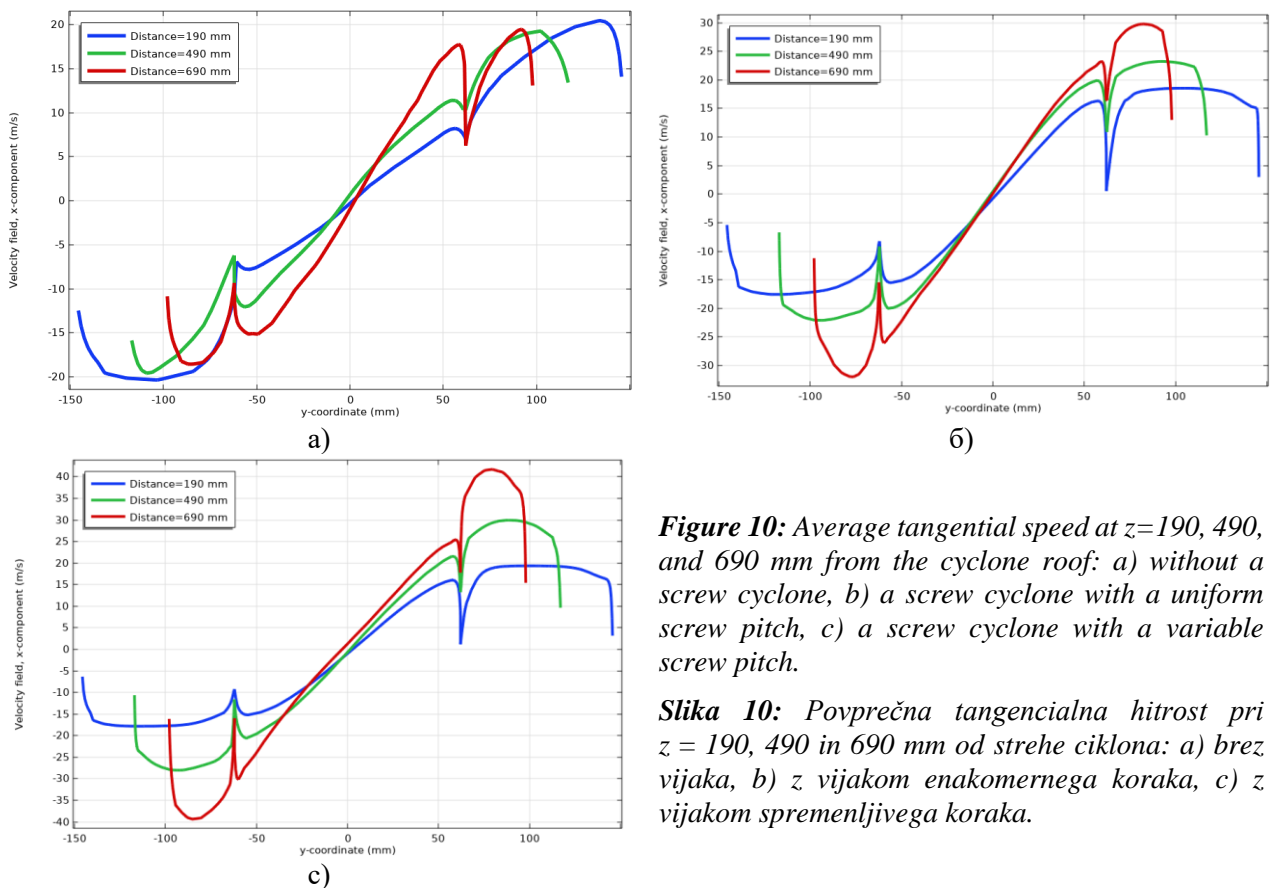


Figure 10: Average tangential speed at $z=190, 490,$ and 690 mm from the cyclone roof: a) without a screw cyclone, b) a screw cyclone with a uniform screw pitch, c) a screw cyclone with a variable screw pitch.

Slika 10: Povprečna tangencialna hitrost pri $z = 190, 490$ in 690 mm od strehe ciklona: a) brez vijaka, b) z vijakom enakomernega koraka, c) z vijakom spremenljivega koraka.

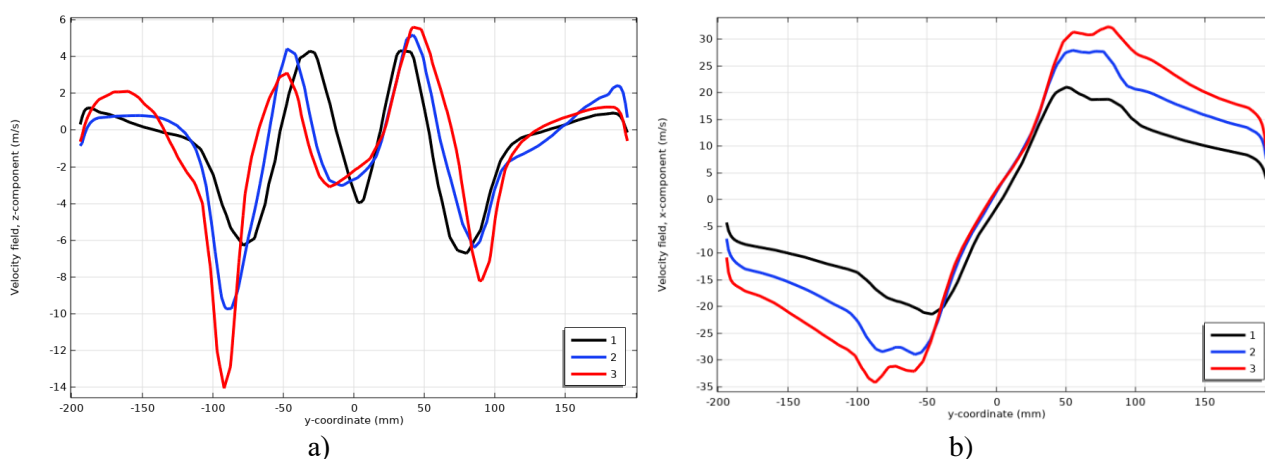


Figure 11: Average axial a) and tangential b) velocities at $z=720$ mm from the cyclone roof. 1 – without a screw cyclone, 2 – a screw cyclone with a uniform screw pitch, 3 – a screw cyclone with a variable screw pitch.

Slika 11: Povprečne aksialne a) in tangencialne b) hitrosti pri $z = 720$ mm od strehe ciklona: 1 – brez vijaka, 2 – z vijakom enakomernega koraka, 3 – z vijakom spremenljivega koraka.

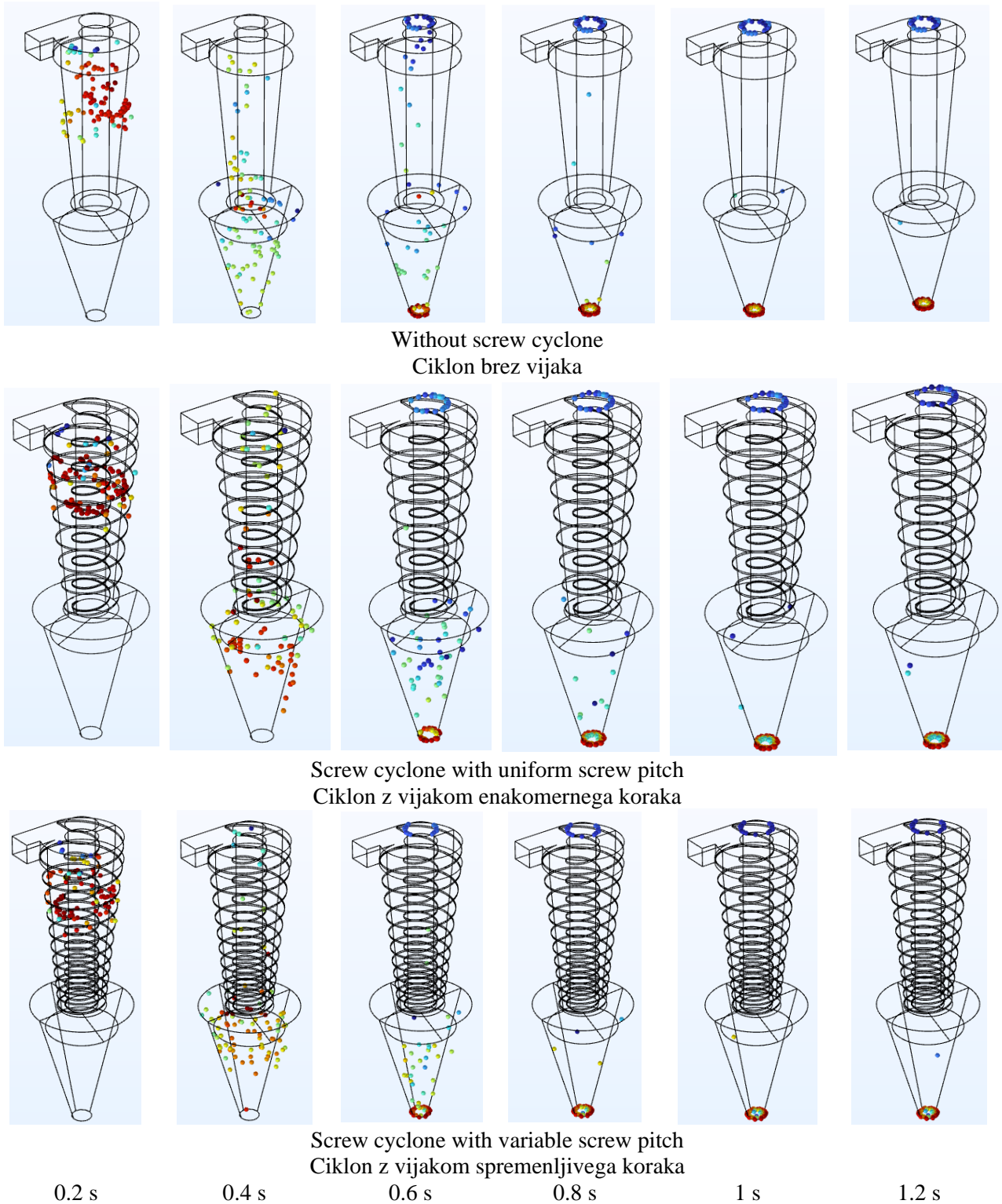


Figure 12: Particle movements at different times. Here the colors represent the particle's velocity at the indicated moment.

Slika 12: Gibanje delcev ob različnih časih. Barve predstavljajo hitrost delca v določenem trenutku.

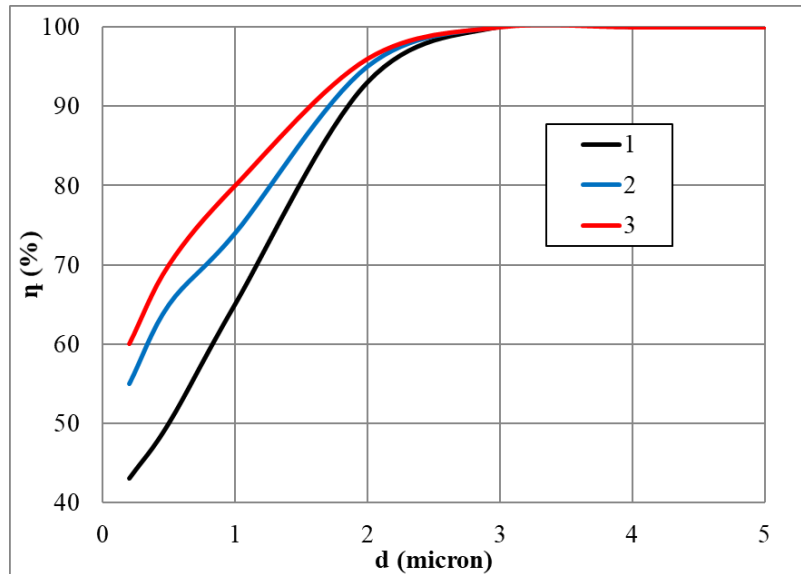


Figure 13: Percentage of lagging particles in cyclones at velocity $U_0 = 18 \text{ m/s}$. 1 – without a screw cyclone, 2 – a screw cyclone with a uniform screw pitch, 3 – a screw cyclone with a variable screw pitch.

Slika 13: Odstotek zaostalih delcev v ciklonih pri hitrosti $U_0 = 18 \text{ m/s}$. 1 – brez vijaka, 2 – z vijakom enakomernega koraka, 3 – z vijakom spremenljivega koraka.

Fig. 6 shows isolines and tangential velocities in cyclones. Fig. 7 shows isolines and radial velocities in cyclones. Figures 5–7 clearly show that, when using a screw (screw cyclone with uniform screw pitch), both the tangential and transverse speeds of the cyclone in Figure 6b increase by 40%. Similarly, when using a screw (screw cyclone with variable screw pitch) in Figure 6c, the tangential speeds increase by 60%. This leads to an increase in centrifugal force. Fig. 8 shows isolines and pressure in cyclones. Fig. 8 shows that the pressure drop without a screw is 722 Pa, 1457 Pa when using a screw cyclone with a uniform screw pitch, and 3115 Pa when using a screw cyclone with a variable screw pitch. Fig. 9 shows the average axial velocity at $z=190, 490,$ and 690 mm from the cyclone roof. Fig. 10 shows the average tangential speed at $z=190, 490,$ and 690 mm from the cyclone roof. Fig. 10 also shows that the tangential speed increases after inserting the screw. Fig. 11 shows the average axial and tangential velocities at $z=720 \text{ mm}$ from the cyclone roof. Fig. 12 illustrates particle movement over time in the upper part of the cyclones, with colors indicating their sizes, based on the inlet velocity $U_0 = 18 \text{ m/s}$. Fig. 13 illustrates the percentage of outgoing dust particles for different

size fractions at the inlet air velocity $U_0 = 18 \text{ m/s}$

. Fig. 13 demonstrates that the efficiency of a screw cyclone (with a uniform screw pitch) for particles with a diameter of $0.1 \mu\text{m}$ is 27%, for particles with a diameter of $0.5 \mu\text{m}$ – 30%, and for particles with a diameter of $1 \mu\text{m}$ – 13%. This type of cyclone is better at collecting zinc particles than cyclones without an auger. On the other hand, the efficiency of a screw cyclone (with variable screw pitch) for particles with a diameter of 0.1 microns is 39%, for particles with a diameter of 0.5 microns 40%, and for particles with a diameter of 1 microns 23%. This cyclone option also captures zinc particles better than a cyclone without an auger. Conclusion: When using a screw cyclone (with variable screw pitch), particle retention is 15% more effective than with other types of cyclones. Thus, the use of a screw cyclone is economically justified in those applications where high separation efficiency is critical. However, if lower operating costs are required, two- or multi-stage screwless cyclones may be a more suitable option. A more detailed economic analysis taking into account the specific application is necessary to make a decision.

2.6 Conclusions

This work used the Comsol Multiphysics 5.6 software package to simulate the aerodynamic processes of two-phase flow inside cyclones. In this case, the SST turbulence model was used. This model should be used to calculate internal flows in systems with curved boundaries, for example, when modeling separator cyclones. Based on the presented data, we can conclude that the use of a screw cyclone, especially with a variable screw pitch, significantly increases the efficiency of collecting zinc particles. Compared to traditional cyclones, auger cyclones show significant improvement in the retention of particles ranging from 0.1 μm to 1 μm in diameter. This indicates the potential of auger cyclones to improve the filtration and purification processes of gas streams, especially with regard to the removal of zinc particles.

References

- Agullo, E., Giraud, L., Guermouche, A., Haidar, A., Roman, J. (2013). Parallel algebraic domain decomposition solver for the solution of augmented systems. *Adv. Eng. Softw.* **60**, 23–30. <https://doi.org/10.1016/j.advengsoft.2012.07.004>.
- Avci, A., Karagoz, I. (2003). Effects of flow and geometrical parameters on the collection efficiency in cyclone separators. *J. Aerosol Sci.* **34**(7), 937–955. [https://doi.org/10.1016/S0021-8502\(03\)00054-5](https://doi.org/10.1016/S0021-8502(03)00054-5).
- Brar, L. S., Sharma, R. P., Dwivedi, R. (2015). Effect of vortex finder diameter on flow field and collection efficiency of cyclone separators. *Part. Sci. Technol.* **33**(1), 34–40. <https://doi.org/10.1080/02726351.2014.933144>.
- Chuah, T. G., Gimbin, J., Choong, T. S. Y. (2006). A CFD study of the effect of cone dimensions on sampling aerocyclones performance and hydrodynamics. *Powder Technol.* **162**(2), 126–132. <https://doi.org/10.1016/j.powtec.2005.12.010>.
- “COMSOL Modeling Software”. COMSOL.com. Comsol, Inc. Retrieved [WWW Document] (2015).
- Hoekstra, A. J. (2000). Gas flow field and collection efficiency of cyclone separators. *TU Delft, Ph. D. Thesis, Delft Univ. Technol.*
- Hoffmann, A. C., De Groot, M., Peng, W., Dries, H. W. A., Kater, J. (2001). Advantages and risks in increasing cyclone separator length. *AIChE J.* **47**(11), 2452–2460. <https://doi.org/10.1002/aic.690471109>.
- Hsu, C.-W., Huang, S.-H., Lin, C.-W., Hsiao, T.-C., Lin, W.-Y., Chen, C.-C. (2014). An experimental study on performance improvement of the stairmand cyclone design. *Aerosol Air Qual. Res.* **14**(3), 1003–1016. <https://doi.org/10.4209/aaqr.2013.04.0129>.
- Kuzmin, D., Löhner, R., Turek, S. (2012). Flux-corrected transport: principles, algorithms, and applications. Springer Science & Business Media.
- Lee, J. W., Yang, H. J., Lee, D. Y. (2006). Effect of the cylinder shape of a long-coned cyclone on the stable flow-field establishment. *Powder Technol.* **165**(1), 30–38. <https://doi.org/10.1016/j.powtec.2006.03.011>.
- Malikov, Z. M., Madaliev, M. E. (2020). Numerical Simulation of Two-Phase Flow in a Centrifugal Separator. *Fluid Dyn.* **55**(8), 1012–1028. <https://doi.org/10.1134/S0015462820080066>.
- Menter, F. R. (1994). Two-equation eddy-viscosity turbulence models for engineering applications. *AIAA J.* **32**(8), 1598–1605. <https://doi.org/10.2514/3.12149>.
- Smirnov, P. E., Menter, F. R. (2009). Sensitization of the SST turbulence model to rotation and curvature by applying the Spalart–Shur correction term. *J. Turbomach.* **131**(4), 041010. <https://doi.org/10.1115/1.3070573>.
- Son, E., Murodil, M. (2020). Numerical calculation of an air centrifugal separator based on the SARC turbulence model. *J. Appl. Comput. Mech.* **6**(Special Issue), 1133–1140. <https://doi.org/10.22055/jacm.2020.31423.1871>.
- Spalart, P. R., Rumsey, C. L. (2007). Effective inflow conditions for turbulence models in aerodynamic calculations. *AIAA J.* **45**(10), 2544–2553. <https://doi.org/10.2514/1.29373>.
- Surmen, A., Avci, A., Karamangil, M. I. (2011). Prediction of the maximum-efficiency cyclone length for a cyclone with a tangential entry. *Powder Technol.* **207**(1–3), 1–8. <https://doi.org/10.1016/j.powtec.2010.10.002>.
- Wei, J., Zhang, H., Wang, Y., Wen, Z., Yao, B., Dong, J. (2017). The gas-solid flow characteristics of cyclones. *Powder Technol.* **308**, 178–192. <https://doi.org/10.1016/j.powtec.2016.11.044>.
- Xiang, R. B., Lee, K. W. (2005). Numerical study of flow field in cyclones of different height. *Chem. Eng. Process. Process Intensif.* **44**(8), 877–883. <https://doi.org/10.1016/j.cep.2004.09.006>.
- Zhu, Y., Lee, K. W. (1999). Experimental study on small

cyclones operating at high flowrates. *J. Aerosol Sci.* **30(10)**, 1303–1315. [https://doi.org/10.1016/S0021-8502\(99\)00024-5](https://doi.org/10.1016/S0021-8502(99)00024-5).

Zlochevsky, V. L., Mukhopad, K. A. (2015). Analysis of air flow formation in a cyclone. *South Siberian Scientific Bulletin* (4), 5–13.

Kuznetsov, S. I., Mikhailik, V. D., Rusanov, S. A. (2009). Modeling the operation of a highly efficient cyclone-rotary dust collector. *Bulletin of Kherson National Technical University* (3), 36.

Tarasova, L. A. (2010). Improving the technological efficiency of vortex-type devices in gas cleaning systems (Doctoral dissertation, Moscow State University of Environmental Engineering).